

UT-19-29  
December, 2019

# Determining Wino Lifetime in Supersymmetric Model at Future 100 TeV $pp$ Colliders

So Chigusa<sup>a</sup>, Yusuke Hosomi<sup>a</sup>, Takeo Moroi<sup>a</sup> and Masahiko Saito<sup>b</sup>

<sup>a</sup>*Department of Physics, University of Tokyo, Tokyo 113-0033, Japan*

<sup>b</sup>*International Center for Elementary Particle Physics, University of Tokyo,  
Tokyo 113-0033, Japan*

## Abstract

We discuss a possibility to measure the lifetime of charged Wino in supersymmetric model at future 100 TeV  $pp$  colliders, assuming that (neutral) Wino is the lightest superparticle (LSP). In the Wino LSP scenario, the charged Wino has a lifetime of about 0.2 ns, and its track may be reconstructed in particular by the inner pixel detectors. We show that the lifetime of charged Wino may be measured by using the information about the distribution of the flight lengths of charged Winos. We propose a procedure for the lifetime determination and show how the accuracy changes as we vary the mass spectrum of superparticle. We also discuss the effects of the detector layouts on the lifetime determination.

# 1 Introduction

Low energy supersymmetry (SUSY), with superparticles at the mass scale much lower than the Planck scale, has been attracted attentions. Even though no direct evidence of superparticles has been experimentally found yet, it is still a well-motivated candidate of physics beyond the standard model. In particular, in models with low energy supersymmetry, gauge coupling unification at the scale of grand unified theory (GUT), i.e.,  $\sim 10^{16}$  GeV, is possible. In addition, more importantly for our study, the lightest superparticle (LSP) in SUSY model with  $R$ -parity conservation can be dark matter. The SUSY dark matter is an important target not only of direct detection experiments but also of high energy colliders. Notably, the collider phenomenology of SUSY dark matter depends on the properties of the LSP.

In the present study, we concentrate on SUSY model in which Winos, which are superpartners of  $SU(2)_L$  gauge bosons, are lighter than other superparticles and discuss its collider phenomenology. This class of model is motivated by the present constraints on low energy SUSY. First, the neutral Wino can be a viable candidate of dark matter. In addition, the Wino LSP naturally shows up from so-called minimal gravity mediation model [1, 2, 3] based on anomaly mediation [4, 5]. In such a model, masses of gauginos are of the order of  $(0.1 - 1)$  TeV, while those of other superparticles are a few orders of magnitude heavier. Notably, such a mass spectrum is well motivated from the Higgs mass point of view because heavier superparticles, in particular heavy stops, can push up the Higgs mass to the observed value of about 125 GeV via radiative corrections [6, 7, 8, 9].

In the SUSY model of our interest, the primary targets of the collider study are Winos as well as other gauginos. The thermal relic abundance of Wino becomes equal to the dark matter density if its mass is about 2.9 TeV [10], while lighter Wino can also become dark matter if Winos are non-thermally produced in the early universe [5, 11]. Combined with the present collider bounds on superparticles, it may be the case that the Winos (and other superparticles) are out of the kinematic reach of the LHC experiment. Such a possibility motivates us to consider more energetic colliders than the LHC. In particular,  $pp$  colliders with the center of mass energy of  $\sim 100$  TeV, called future circular collider (or FCC-hh), is now seriously discussed.

Here, we consider the collider phenomenology of supersymmetric model with Wino LSP at FCC-hh. In the previous studies, it has been discussed that the discovery [12] and the mass measurements [13] of gauginos are possible at FCC-hh, particularly relying on the existence of disappearing tracks of charged Winos.<sup>#1</sup> In the case of Wino LSP, it is often the case that the mass difference between charged and neutral Winos is induced dominantly by the radiative correction due to the electroweak gauge bosons; the charged Wino becomes slightly heavier than the neutral one and the mass difference is given by  $\sim 160$  MeV. As a result, the charged Wino becomes fairly long-lived; its lifetime is often  $\sim 0.2$  ns and is insensitive to the mass spectrum of superparticles (as far as superparticles other than gauginos are much heavier than Wino). Then, once produced at the colliders, the charged Wino may fly

---

<sup>#1</sup>We may also use the study of mono-jet events [14] and precision study of the Drell-yan processes [15, 16, 17, 18] for the discovery of the signals of electroweakly interacting particles, like Winos, at the FCC-hh.

$O(1 - 10)$  cm and may be identified as a short high  $p_T$  track. In order to understand the properties of Winos, measurement of the lifetime of charged Wino is an important step.

In this letter, we study the possibility of measuring the lifetime of charged Wino at FCC-hh. If the Wino mass is less than  $\sim 2.9$  TeV, which is the upper bound on the Wino mass from the point of view of dark matter, it is expected that the charged Wino is within the reach of FCC-hh [12] and that the Wino mass can be determined [13]. Here, using SUSY events with charged Wino production, we show that the lifetime of the charged Wino can be also determined. We discuss the basic procedure to determine the charged Wino lifetime at FCC-hh, and show the expected accuracy of the lifetime measurement. The organization of this letter is as follows. In Section 2, we explain the method of the lifetime measurements at the FCC-hh. We also summarize important features of the model of our interest. Then, in Section 3, we show our numerical results. Section 4 is devoted for conclusions and discussion.

## 2 Formalism

Let us explain the setup of our analysis. Here, we concentrate on supersymmetric models in which Winos are lighter than other supersymmetric particles. Detailed mass spectrum of superparticles for our Monte Carlo (MC) analysis will be explained in the next section. We also assume that the mass difference between the charged and neutral Winos dominantly comes from radiative effects due to electroweak gauge bosons. In such models, neutral Wino becomes slightly lighter than charged ones, and hence neutral Wino becomes the LSP while charged Wino becomes long-lived. The mass difference is predicted to be  $\sim 160$  MeV which gives the lifetime of the charged Wino of  $\sim 0.2$  ns [19, 20, 21, 22, 23]. Here, we take the canonical lifetime of charged Wino to be  $c\tau = 5.75$  cm [23], with  $c$  being the speed of light. In the following, we study how well we can determine the lifetime of charged Wino at the FCC-hh experiment. Although our primary interest is to determine the Wino lifetime, we vary the input value of the lifetime to see how the sensitivity depends on it.

Once produced, charged Wino travels finite distance and decays into neutral Wino (and charged pion). In particular, some of charged Winos travel long enough to go through several layers of inner pixel detectors and to be reconstructed as (disappearing) tracks. Such disappearing tracks can be used not only for the reduction of standard model backgrounds but also for the determination of the lifetime of charged Wino.

Expecting that there exist several layers of pixel detectors, let  $\tilde{W}_i^\pm$  ( $i = 1 - n_A$ ) be charged Winos which arrive  $A$ -th layer of the pixel detector before decaying. Here,  $n_A$  is the number of charged Wino samples available for the lifetime measurement. Then, the expectation value of the number of charged Winos which arrive  $B$ -th layer ( $B > A$ ) is

$$\langle n_B \rangle(\tau) = \sum_{i=1}^{n_A} p_i(\tau), \quad (2.1)$$

with

$$p_i(\tau) \equiv e^{-(L_T^{(B)} - L_T^{(A)})/\tau\beta_i\gamma_i \sin\theta_i}, \quad (2.2)$$

where  $L_T^{(A)}$  and  $L_T^{(B)}$  are transverse distance from the interaction point to the  $A$ - and  $B$ -th layers, respectively,  $\beta_i$  is the velocity of  $i$ -th Wino,  $\gamma_i \equiv 1/\sqrt{1-\beta_i^2}$ , and  $\theta_i$  is the angle between the proton beam and the direction of the momentum of  $\tilde{W}_i^\pm$ . Notice that  $\langle n_B \rangle$  is an increasing function of  $\tau$  and is sensitive to the lifetime of charged Wino. Thus, with the measurements of the numbers of charged Winos arriving at  $A$ - and  $B$ -th layers, we may acquire information about  $\tau$ , assuming that the velocity and the propagation direction of charged Winos are measurable. In particular, once  $n_B$  (i.e., the number of charged Winos reaching to the  $B$ -th layer) is measured, the best-fit value of the lifetime is given by solving

$$\langle n_B \rangle(\tau^{(\text{best})}) = n_B. \quad (2.3)$$

The propagations of charged Winos from the  $A$ -th layer to the  $B$ -th are multiples of Bernoulli processes with various probabilities. Assuming a test lifetime  $\tau^{(\text{test})}$ , the probability to realize a specific value of  $n_B$  for a given data set is expressed as [24]

$$\begin{aligned} P(n_B; \tau^{(\text{test})}) &= \left[ \prod_{i=1}^{n_A} (1 - p_i^{(\text{test})}) \right] \sum_{i_1 < i_2 < \dots < i_{n_B}} \left[ \frac{p_{i_1}^{(\text{test})}}{1 - p_{i_1}^{(\text{test})}} \frac{p_{i_2}^{(\text{test})}}{1 - p_{i_2}^{(\text{test})}} \dots \frac{p_{i_{n_B}}^{(\text{test})}}{1 - p_{i_{n_B}}^{(\text{test})}} \right], \\ &= \frac{1}{n_A + 1} \sum_{l=0}^{n_A} e^{-2\pi i n_A l / (n_A + 1)} \prod_{k=1}^{n_A} \left[ 1 + (1 - e^{2\pi i l / (n_A + 1)}) p_k^{(\text{test})} \right]. \end{aligned} \quad (2.4)$$

where  $p_i^{(\text{test})} \equiv p_i(\tau^{(\text{test})})$  and the sum is taken for all the possible sets of  $\{i_1, i_2, \dots, i_{n_B}\}$ . The second equality follows from [25], which reduces the cost of numerical calculation.

Once charged Winos are observed at future collider experiments with the measurements of their velocities and directions (as well as  $n_A$  and  $n_B$ ), we may constrain the lifetime of charged Wino. In our analysis, we define  $\alpha$  % “confidence interval,” which we denote  $\{n_B\}_\alpha$ , as follows. We define integers  $I_1, \dots, I_{n_A}$  such that  $P(I_1; \tau^{(\text{test})}) \geq \dots \geq P(I_{n_A}; \tau^{(\text{test})})$ . Then, the confidence interval,  $\{n_B\}_\alpha \equiv \{I_1, \dots, I_N\}$ , is defined as

$$\sum_{I \in \{n_B\}_\alpha} P(I; \tau^{(\text{test})}) - P(I_N; \tau^{(\text{test})}) < \alpha \% \leq \sum_{I \in \{n_B\}_\alpha} P(I; \tau^{(\text{test})}). \quad (2.5)$$

A test lifetime  $\tau^{(\text{test})}$  is allowed (excluded) if observed  $n_B$  is inside (outside) of the confidence interval calculated with  $\tau^{(\text{test})}$ . In the next section, we discuss how well we can determine the lifetime using MC analysis.

### 3 Monte Carlo Analysis

In this section, we show that the determination of the lifetime of charged Wino is really possible using MC analysis. For simplicity, motivated by the minimal gravity mediation model based on anomaly mediation, we concentrate on the model in which gauginos (i.e., Bino, Wino, and gluino) are the only superparticles accessible with FCC-hh; other superparticles

	Point 1	Point 2	Point 3
$m_{\tilde{B}}$ [GeV]	3660	4060	4470
$m_{\tilde{W}}$ [GeV]	2900	2900	2900
$m_{\tilde{g}}$ [GeV]	6000	7000	8000
$\sigma(pp \rightarrow \tilde{g}\tilde{g})$ [fb]	7.9	2.7	1.0
$\mathcal{L}$ [1/ab]	10	10	30

Table 1: Gaugino masses and the gluino pair production cross section (for the center-of-mass of 100 TeV) for the Sample Points 1, 2, and 3. We also show the canonical luminosities used for the analysis for these Sample Points.

are assumed to be too heavy to be produced. In addition, Winos are assumed to be lighter than Bino and gluino. We adopt three Sample Points which are based on the minimal gravity mediation model [13]. The Sample Points are shown in Table 1; on the table, the masses of Bino, Wino, and gluino (denoted as  $m_{\tilde{B}}$ ,  $m_{\tilde{W}}$ , and  $m_{\tilde{g}}$ , respectively) as well as the gluino pair production cross section and the canonical luminosity in our analysis are given. In our study, we take  $\text{Br}(\tilde{g} \rightarrow \tilde{W}\bar{q}q) = \text{Br}(\tilde{g} \rightarrow \tilde{B}\bar{q}q) = 0.5$  (with  $q$  being quarks), with the assumption of the flavor universality of the final-state quarks. For the cases of the gluino mass of 6 and 7 TeV, we assume the integrated luminosity of  $\mathcal{L} = 10 \text{ ab}^{-1}$ , while  $\mathcal{L} = 30 \text{ ab}^{-1}$  is used for the case of  $m_{\tilde{g}} = 8 \text{ TeV}$  to compensate the smallness of the gluino production cross section.

Our method of event generation is mostly the same as that adopted in [13]. We use `MadGraph5_aMC@NLO` [26, 27] for the generation of  $pp \rightarrow \tilde{g}\tilde{g}$  and  $pp \rightarrow \tilde{W}^+\tilde{W}^- + \text{jets}$  events. The results are passed to `PYTHIA8` [28] for the decay and hadronization processes. Then, `Delphes` (v3.4.1) [29] is used for a fast detector simulation; we use the card `FCCh.tcl` included in the package. The velocities of charged Winos are smeared by our original code. We expect that, at FCC-hh, the charged Wino track can be reconstructed and that information about the time of flight is available if the charged Wino hits several layers of pixel detector. We assume 6 % error in the velocity measurement [13]; for reconstructed charged Wino tracks, the observed values of the Wino velocity are determined as follows:

$$\beta = (1 + 6 \% \times Z)\beta^{(\text{true})}, \quad (3.1)$$

where  $\beta$  and  $\beta^{(\text{true})}$  are observed and true values of the velocity and  $Z$  is the  $(0, 1)$  Gaussian random variable. We neglect the error in the measurement of the directions of Wino tracks.

In the following analysis, we assume that the charged Winos are required to hit at least inner four layers of the pixel detector for the track reconstruction (and also for background reduction). In order to eliminate standard model backgrounds, we use only the events satisfying the following requirements:

1. There exist two ‘‘long enough’’ Wino-like tracks. The transverse length of the tracks should be longer than the transverse distance to the 4th pixel detector  $L_T^{(4)}$ . In addition, the pseudo-rapidities ( $\eta$ ) of the tracks should satisfy  $|\eta| < 1.5$ .

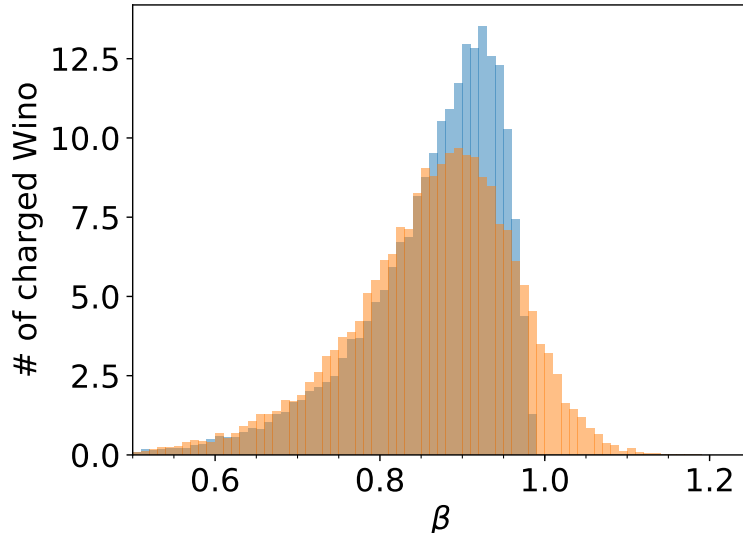


Figure 1: Distributions of the true (blue) and observed (orange) velocities of charged Winos for the Sample Point 1. The height of the histogram is the number of charged Winos in the bin for events satisfying the Requirements 1 and 2. The bin width is  $\Delta\beta = 0.01$ .

2. The missing transverse energy (MET) should be larger than 1 TeV.

With these requirements, we expect that the standard model backgrounds can become negligible, as discussed in [13].

In Fig. 1, we show the distribution of  $\beta$  and  $\beta^{(\text{true})}$  for the Sample Point 1, using the events satisfying Requirements 1 and 2. (Here, 100 sets of the event samples are used for the figure.) We can see that the peak of the distribution is shifted to the small value of the velocity after the smearing. We will discuss its effects of the lifetime determination later.

For the determination of  $\tau$ , we use charged Winos in the events satisfying the requirements given above, and hence we take  $(A, B) = (4, 5)$ . In addition, for the lifetime determination, velocity information about charged Winos is necessary. In order for a good velocity measurement, we use only charged Winos whose (observed) velocity is smaller than 0.85 for the lifetime determination.

First, we consider the case where the gluino mass is light enough so that the gluino pair production dominates the SUSY events at FCC-hh (i.e., the case of the Sample Points 1 – 3). In Fig. 2, taking  $L_T^{(4)} = 10$  cm and  $L_T^{(5)} = 15$  cm, we plot  $P(n_5; \tau^{(\text{test})})$  taking  $c\tau^{(\text{test})} = 3$  cm (blue),  $c\tau^{(\text{test})} = 5.75$  cm (red), and  $c\tau^{(\text{test})} = 10$  cm (green), using the event sample generated from the Sample Point 1 with  $c\tau = 5.75$  cm. We can see that the behavior of  $P(n_5; \tau^{(\text{test})})$  is strongly dependent on  $\tau^{(\text{test})}$ . Thus, with the measurement of the number of charged Winos reaching to the 5th layer, we can obtain information about the lifetime. We also plot the Gaussian distribution  $N(\hat{n}_5(\tau^{(\text{test})}), \hat{n}_5(\tau^{(\text{test})}))$ , where  $\hat{n}_5(\tau^{(\text{test})})$  is the value

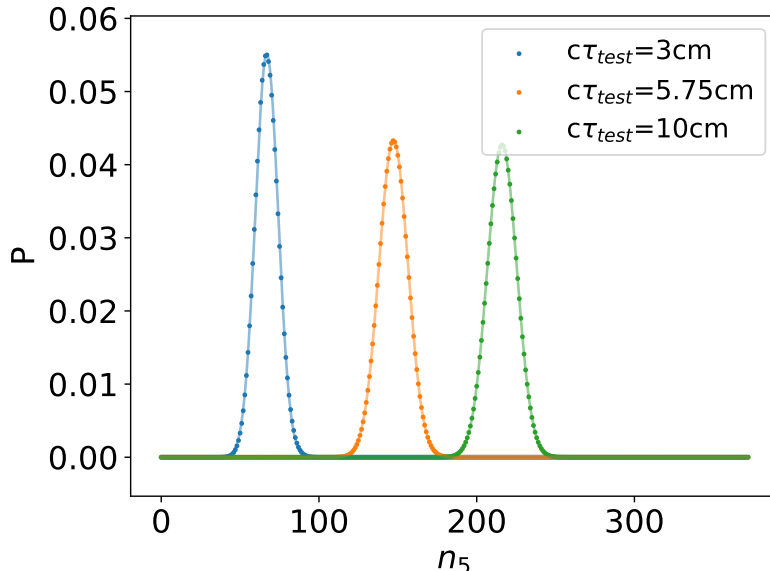


Figure 2: The dots show  $P(n_5; \tau^{(\text{test})})$  for  $L_T^{(4)} = 10$  cm and  $L_T^{(5)} = 15$  cm, using the event samples generated from the Sample Point 1 with  $c\tau = 5.75$  cm.  $c\tau^{(\text{test})}$  is taken to be 3 cm (blue), 5.75 cm (red), and 10 cm (green) from left to right. The solid lines show the Gaussian distribution  $N(\hat{n}_5(\tau^{(\text{test})}), \hat{n}_5(\tau^{(\text{test})}))$ , where  $\hat{n}_5(\tau^{(\text{test})})$  is the value of  $n_5$  which maximizes  $P(n_5; \tau^{(\text{test})})$ .

of  $n_5$  which maximizes  $P(n_5; \tau^{(\text{test})})$ . We can see that the probability distribution is well approximated by the Gaussian distribution when the number of charged Winos reaching to the 5th layer is large enough.

In Figs. 3 – 5, we plot the best-fit value of the lifetime as well as the expected lower and upper bounds for various choices of  $\tau$  for the Sample Points 1 – 3. Here, we use 100 independent data sets for each Sample Point, and determine the lower and upper bounds on the lifetime for each data set using the probability distribution defined in Eq. (2.4). The expected lower and upper bounds shown in the figures are obtained by taking the median of those from 100 independent data sets. The regions with  $\tau$  giving rise to  $\langle n_4 \rangle < 10$ , for which our method of the lifetime measurement becomes difficult, are shaded.

We can see that the best-fit values of the lifetime are systematically overestimated in the present analysis. This is mainly due to the error in the velocity measurement. Here, the Wino velocity is assumed to be measured with the 6 % accuracy (see Eq. (3.1)). As one can see in Fig. 1, the observed Wino velocity is likely to be smaller than the true value, resulting in the overestimation of the lifetime. We checked that the best-fit values become consistent with the input values if the true value of the Wino velocity is used in the analysis. We assume that such a systematic effect originating from the velocity measurement can be well understood in the actual experiment. Thus, we will not include the shift of the best-fit value in estimating the uncertainty of the lifetime determination.

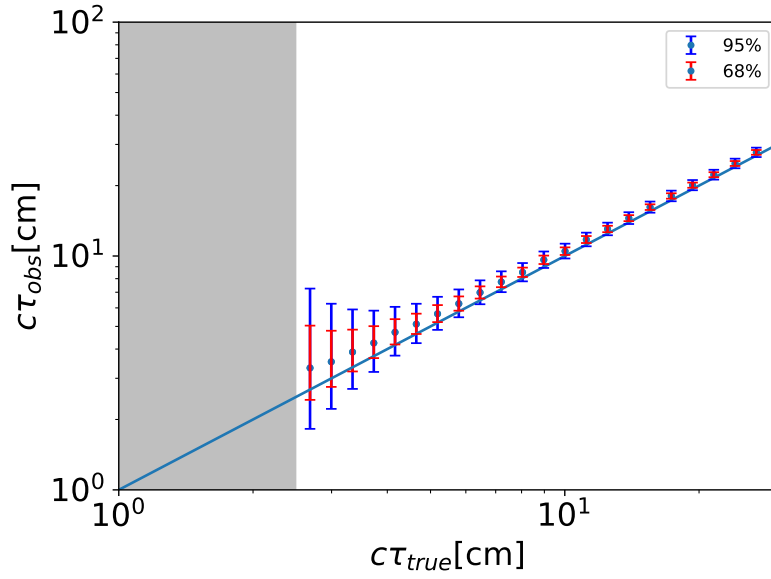


Figure 3: Expected 68% and 95% confidence level lower and upper bounds from the lifetime measurements, as well as the best-fit values, for the Sample Point 1.

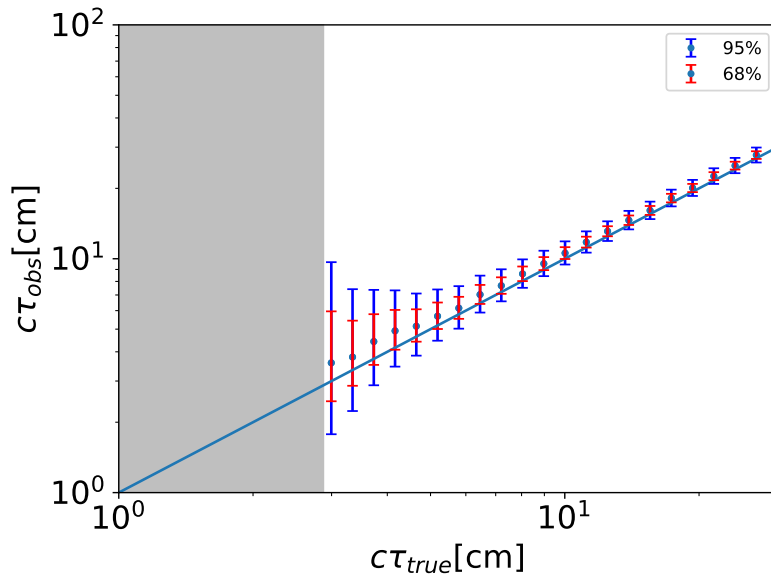


Figure 4: Same as Fig. 3, except for the Sample Point 2.

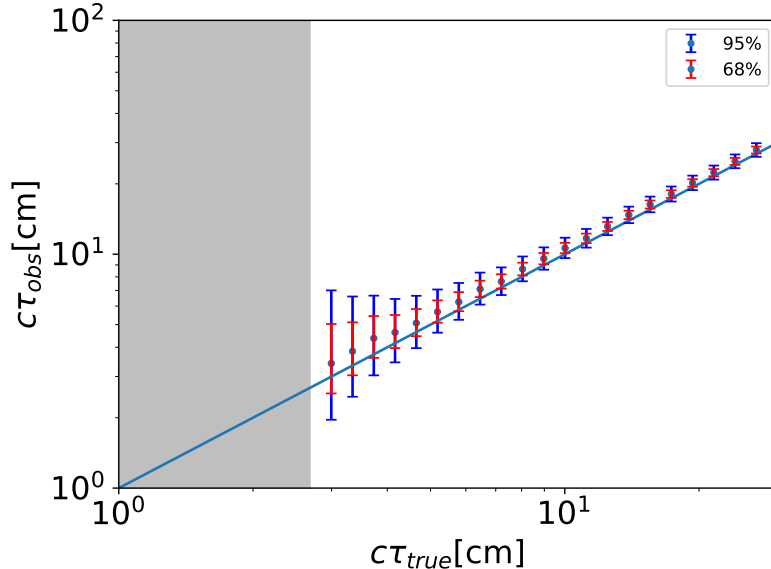


Figure 5: Same as Fig. 3, except for the Sample Point 3.

Next, we show how the accuracy of the lifetime determination depends on the detector layouts. The accuracy depends on the distances to the pixel layers. In Fig. 6, for the Sample Point 1 with taking  $c\tau = 5.75$  cm, we show the expected lower and upper bounds for several choices of the distances to the layers. As expected, the accuracy becomes worse as the distances to the 4th layer becomes longer; with larger  $L_T^{(4)}$ , the number of charged Winos available for the analysis becomes smaller.

We define the uncertainties in the lifetime determination as

$$\delta\tau^{(\pm)} \equiv |\tau^{(\pm)} - \tau^{(\text{best})}|, \quad (3.2)$$

where  $\tau^{(-)}$  and  $\tau^{(+)}$  are lower and upper bounds on the lifetime for a given confidence interval, respectively. For the Sample Points 1 – 3 with  $c\tau = 5.75$  cm, the values of  $\tau^{(\pm)}$  for several choices of detector layouts are summarized in Table 2. In the same Table, we show the median values of  $n_4$  and  $n_5$  for each detector layout. For some sample points,  $n_4$  for  $(L_T^{(4)}, L_T^{(5)}) = (15 \text{ cm}, 20 \text{ cm})$  and that for  $(15 \text{ cm}, 27 \text{ cm})$  slightly differ; it is due to statistical fluctuations.

When gluino is too heavy to be produced, the gluino pair production process cannot be used for our analysis. Even in such a case, we may use the direct production of Winos for the lifetime determination. In particular, if the Wino mass is  $\sim 2.9$  TeV, which is the value of the Wino mass relevant for the thermal Wino dark matter scenario, charged Wino can be within the discovery reach of the disappearing track search at the FCC-hh [12]. This fact indicates that the lifetime determination is also possible. In order to see how well we can determine the lifetime, we consider the process  $pp \rightarrow \tilde{W}^+ \tilde{W}^- + \text{jets}$ . Here, the extra jets

Sample Point 1

$(L_T^{(4)}, L_T^{(5)})$	$c\delta\tau^{(-)}$ (68 %)	$c\delta\tau^{(+)}$ (68 %)	$c\delta\tau^{(-)}$ (95 %)	$c\delta\tau^{(+)}$ (95 %)	$n_4$	$n_5$
(10 cm, 15 cm)	0.40	0.45	0.76	0.93	400	180
(11 cm, 15 cm)	0.51	0.57	0.94	1.2	290	150
(15 cm, 20 cm)	0.87	1.1	1.6	2.4	85	40
(15 cm, 27 cm)	0.83	1.2	1.5	2.3	85	16

Sample Point 2

$(L_T^{(4)}, L_T^{(5)})$	$c\delta\tau^{(-)}$ (68 %)	$c\delta\tau^{(+)}$ (68 %)	$c\delta\tau^{(-)}$ (95 %)	$c\delta\tau^{(+)}$ (95 %)	$n_4$	$n_5$
(10 cm, 15 cm)	0.65	0.74	1.2	1.5	170	78
(11 cm, 15 cm)	0.80	0.90	1.4	2.0	120	66
(15 cm, 20 cm)	1.4	1.9	2.3	4.2	38	17
(15 cm, 27 cm)	1.2	1.7	2.1	3.5	40	7

Sample Point 3

$(L_T^{(4)}, L_T^{(5)})$	$c\delta\tau^{(-)}$ (68 %)	$c\delta\tau^{(+)}$ (68 %)	$c\delta\tau^{(-)}$ (95 %)	$c\delta\tau^{(+)}$ (95 %)	$n_4$	$n_5$
(10 cm, 15 cm)	0.56	0.64	1.0	1.3	230	100
(11 cm, 15 cm)	0.71	0.79	1.2	1.6	170	90
(15 cm, 20 cm)	1.1	1.4	2.0	3.2	53	25
(15 cm, 27 cm)	1.0	1.5	1.9	3.3	53	10

 $pp \rightarrow \tilde{W}^+ \tilde{W}^- + \text{jets}$ 

$(L_T^{(4)}, L_T^{(5)})$	$c\delta\tau^{(-)}$ (68 %)	$c\delta\tau^{(+)}$ (68 %)	$c\delta\tau^{(-)}$ (95 %)	$c\delta\tau^{(+)}$ (95 %)	$n_4$	$n_5$
(10 cm, 15 cm)	1.1	1.5	1.9	3.2	60	28
(11 cm, 15 cm)	1.3	1.8	2.2	4.0	45	24
(15 cm, 20 cm)	2.2	3.6	3.4	9.2	15	7
(15 cm, 27 cm)	1.8	3.8	3.2	8.1	15	3

Table 2: The expected uncertainties in the lifetime determination in units of cm, adopting several choices of detector layouts. The input value of the lifetime is taken to be  $c\tau = 5.75$  cm. The median values of  $n_4$  and  $n_5$  are also shown.

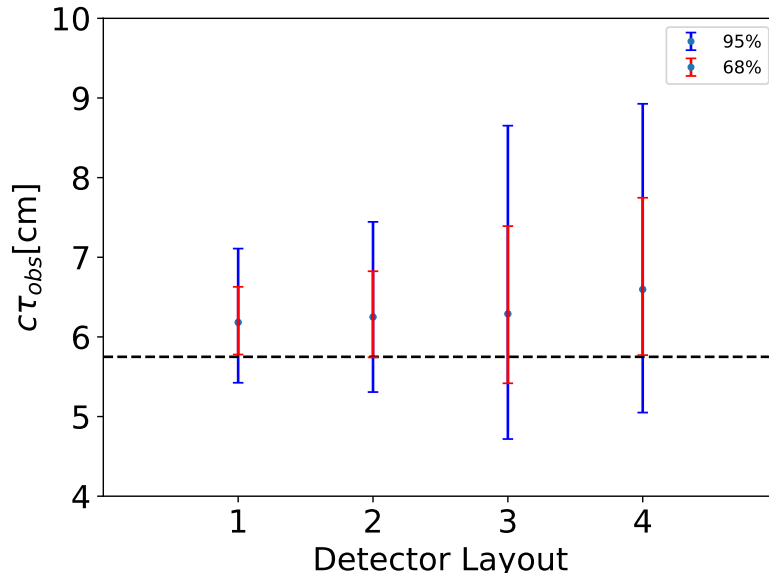


Figure 6: Accuracies of the lifetime determination for several choices of the detector layout for the Sample Point 1 with  $c\tau = 5.75$  cm. Here, we take  $(L_T^{(4)}, L_T^{(5)}) = (10$  cm, 15 cm), (11 cm, 15 cm), (15 cm, 20 cm), and (15 cm, 27 cm) from left to right.

are required for the trigger selection (as well as for the kinematical cut of our choice). For the events, we impose the Requirements 1 and 2, which we mentioned before. Then, using the events satisfying the Requirements, we determine the best-fit value of the lifetime as well as the confidence interval. In Fig. 7, with adopting several detector layouts, we show the expected accuracy of the determination of the Wino lifetime, taking  $m_{\tilde{W}} = 2.9$  TeV,  $c\tau = 5.75$  cm, and  $\mathcal{L} = 30$   $\text{ab}^{-1}$ . Here, we use independent 500 data sets to calculate the median values of best-fit lifetime as well as lower and upper bounds. However  $n_5 = 0$  in 5 data sets of them, so we exclude these sets before taking the median. The uncertainties for our choices of detector layouts are also summarized in Table 2, taking  $c\tau = 5.75$  cm. One can see that the uncertainties are larger than the cases of the gluino pair production events. This is mainly due to the smallness of the cross section for the  $pp \rightarrow \tilde{W}^+ \tilde{W}^- + \text{jets}$  process. Even so, the Wino lifetime can be determined with a relatively good accuracy, i.e.,  $\delta\tau^{(\pm)}/\tau \sim O(10)$  %, in particular if a compact pixel detector with  $L_T^{(5)} \sim 15$  cm is available. We also comment here that, for  $L_T^{(4)} = 15$  cm, the layout with  $L_T^{(5)} = 27$  cm gives better accuracy than  $L_T^{(5)} = 20$  cm. This is due to the fact that the accuracy becomes worse when  $L_T^{(A)}$  and  $L_T^{(B)}$  take too close values.

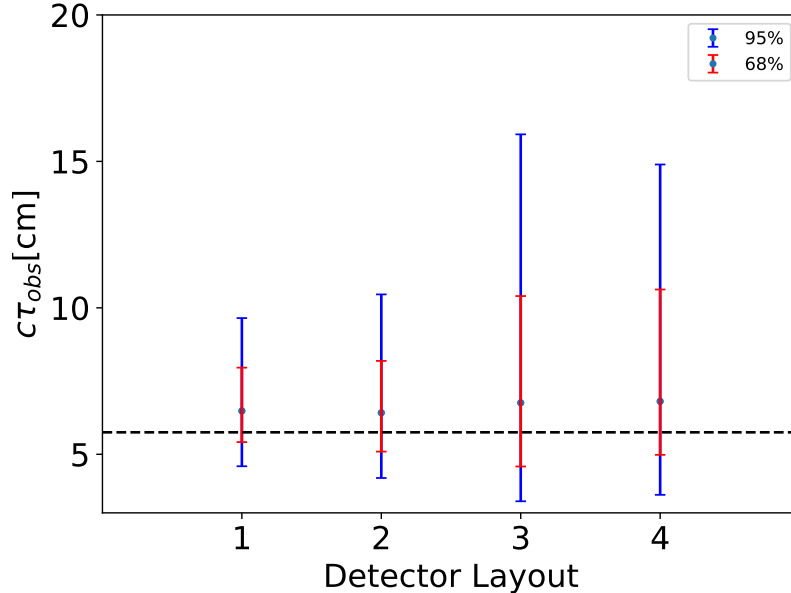


Figure 7: Accuracies of the lifetime determination for several choices of the detector layout for  $m_{\tilde{W}} = 2.9$  TeV and  $c\tau = 5.75$  cm, using the process  $pp \rightarrow \tilde{W}^+ \tilde{W}^- + \text{jets}$ . Here, we take  $(L_T^{(4)}, L_T^{(5)}) = (10 \text{ cm}, 15 \text{ cm}), (11 \text{ cm}, 15 \text{ cm}), (15 \text{ cm}, 20 \text{ cm}),$  and  $(15 \text{ cm}, 27 \text{ cm})$  from left to right.

## 4 Conclusions and Discussion

In this letter, we have discussed the possibility to determine the lifetime of charged Wino in supersymmetric model, assuming that the neutral Wino is the LSP. In such a case, the lifetime of the charged Wino is given by  $c\tau \simeq 5.75$  cm, for which we have seen that a significant number of charged Winos may hit several layers of inner pixel detector and may be used for the lifetime determination. Concentrating on the case with the Wino mass of 2.9 TeV, which is the relevant value to make thermal relic Wino as dark matter, we have studied the prospect of the Wino lifetime determination at FCC-hh.

If gluino is within the kinematical reach of FCC-hh, we may use the charged Winos produced by the decay of gluino. In such a case, the Wino lifetime may be determined with the accuracy of 14 % (30 %) for the 68 % (95 %) confidence interval. Even if gluino is out of the kinematical reach, we may use the charged Winos produced by the process  $pp \rightarrow \tilde{W}^+ \tilde{W}^- + \text{jets}$ . In such a case, the accuracy of the lifetime determination becomes worse, but still it can be 43 % (92 %) for the 68 % (95 %) confidence interval. These measurements of the Wino lifetime provides an important confirmation that the observed charged particle is really  $\tilde{W}^\pm$ .

Finally, we comment on the effects of the accidental alignments of the hits on the pixel detector, which has been neglected in our analysis. Potentially, the most serious effect may come from the hits on the 5th layer near the trajectories of the true charged Wino tracks.

If there exist such hits for charged Winos which decay before reaching 5th layer, they affect the measurement of  $n_5$ . According to the study of the fake tracks given in [12], however, the probability to have fake charged Wino tracks decreases by a factor of  $O(100)$  with requiring a hit on an extra layer. Thus, we estimate that the error of  $n_5$  due to the accidental alignment is less than  $O(10^{-2}) \times n_4$ , which is negligible in the situation of our study.

## Acknowledgments

This work was supported by MEXT KAKENHI Grant number JP16K21730 and JSPS KAKENHI Grant (Nos. 17J00813 [SC], 16H06490 [TM], 18K03608 [TM], and 18J11405 [MS]).

## References

- [1] M. Ibe, T. Moroi and T. T. Yanagida, Phys. Lett. B **644** (2007) 355 [hep-ph/0610277].
- [2] M. Ibe and T. T. Yanagida, Phys. Lett. B **709** (2012) 374 [arXiv:1112.2462 [hep-ph]].
- [3] N. Arkani-Hamed, A. Gupta, D. E. Kaplan, N. Weiner and T. Zorawski, arXiv:1212.6971 [hep-ph].
- [4] L. Randall and R. Sundrum, Nucl. Phys. B **557** (1999) 79 [hep-th/9810155].
- [5] G. F. Giudice, M. A. Luty, H. Murayama and R. Rattazzi, JHEP **9812** (1998) 027 [hep-ph/9810442].
- [6] Y. Okada, M. Yamaguchi and T. Yanagida, Prog. Theor. Phys. **85** (1991) 1.
- [7] H. E. Haber and R. Hempfling, Phys. Rev. Lett. **66** (1991) 1815.
- [8] J. R. Ellis, G. Ridolfi and F. Zwirner, Phys. Lett. B **257** (1991) 83.
- [9] J. R. Ellis, G. Ridolfi and F. Zwirner, Phys. Lett. B **262** (1991) 477.
- [10] J. Hisano, S. Matsumoto, M. Nagai, O. Saito and M. Senami, Phys. Lett. B **646** (2007) 34 [hep-ph/0610249].
- [11] T. Moroi and L. Randall, Nucl. Phys. B **570** (2000) 455 [hep-ph/9906527].
- [12] M. Saito, R. Sawada, K. Terashi and S. Asai, Eur. Phys. J. C **79** (2019) no.6, 469 [arXiv:1901.02987 [hep-ph]].
- [13] S. Asai *et al.*, JHEP **1905** (2019) 179 [arXiv:1901.10389 [hep-ph]].
- [14] T. Han, S. Mukhopadhyay and X. Wang, Phys. Rev. D **98** (2018) no.3, 035026 [arXiv:1805.00015 [hep-ph]].

- [15] S. Chigusa, Y. Ema and T. Moroi, Phys. Lett. B **789** (2019) 106 [arXiv:1810.07349 [hep-ph]].
- [16] L. Di Luzio, R. Gröber and G. Panico, JHEP **1901** (2019) 011 [arXiv:1810.10993 [hep-ph]].
- [17] S. Matsumoto, S. Shirai and M. Takeuchi, JHEP **1903** (2019) 076 [arXiv:1810.12234 [hep-ph]].
- [18] T. Abe, S. Chigusa, Y. Ema and T. Moroi, Phys. Rev. D **100** (2019) no.5, 055018 [arXiv:1904.11162 [hep-ph]].
- [19] H. C. Cheng, B. A. Dobrescu and K. T. Matchev, Nucl. Phys. B **543** (1999) 47 [hep-ph/9811316].
- [20] J. L. Feng, T. Moroi, L. Randall, M. Strassler and S. f. Su, Phys. Rev. Lett. **83** (1999) 1731 [hep-ph/9904250].
- [21] T. Gherghetta, G. F. Giudice and J. D. Wells, Nucl. Phys. B **559** (1999) 27 [hep-ph/9904378].
- [22] Y. Yamada, Phys. Lett. B **682** (2010) 435 [arXiv:0906.5207 [hep-ph]].
- [23] M. Ibe, S. Matsumoto and R. Sato, Phys. Lett. B **721** (2013) 252 [arXiv:1212.5989 [hep-ph]].
- [24] S. X. Chen and J. S. Liu, Statistica Sinica **7** (1997) 875.
- [25] M. Fernandez and S. Williams, IEEE Transactions on Aerospace Electronic Systems **46** (2010) 803.
- [26] J. Alwall, M. Herquet, F. Maltoni, O. Mattelaer and T. Stelzer, JHEP **1106** (2011) 128 [arXiv:1106.0522 [hep-ph]].
- [27] J. Alwall *et al.*, JHEP **1407** (2014) 079 [arXiv:1405.0301 [hep-ph]].
- [28] T. Sjostrand *et al.*, Comput. Phys. Commun. **191** (2015) 159 [arXiv:1410.3012 [hep-ph]].
- [29] J. de Favereau *et al.* [DELPHES 3 Collaboration], JHEP **1402** (2014) 057 [arXiv:1307.6346 [hep-ex]].